 CMES, vol.4, no.2, pp.239-248, 2003

Element Coordinates and the Utility in Large Displacement Analysis of a Space Frame

K. Ijima[1], H. Obiya[1], S. Iguchi[2] and S. Goto[2]

Abstract: Defining element coordinates in space frame, element end deformations become statically clear from the energy principle. Therefore, the deformations can be expressed by nodal displacement without any approximation. The paper indicates that the exact expressions of the deformations and the geometrical stiffness strictly based on the equations makes large displacement analysis of space frame possible with robustness on the computation.

keyword: geometrically nonlinear analysis, large displacement, finite rotation, space frame

1 Introduction

Many researches related to geometrically nonlinear analysis of a space frame have been already published. Though the authors do not grasp all of the researches, it is obvious that FEM plays an important role in the research. Before recognizing the wide usability of FEM, there had been some research [representatively, Oran (1973)], which applied the elemental theory a beam to the geometrically nonlinear analysis. One of the authors also published a similar theory, but more precise in terms of finite rotation [Goto (1983)]. Along growing of popularity of FEM, however, it became a common sense to use displacement functions and Lagarange's formulation including its strain field in the analysis. Bathe and Bolourchi (1979) seems to be the beginning.

In FEM, however, it is quite difficult to obtain the displacement function in which finite rotation is strictly considered. This is because the function has to express total deformation in the element. On the other hand, if the deformations expressed by nodal displacements are restricted at the element ends, the end deformations are obtained by introducing the element coordinates without any approximation. The element coordinates are not only used for transforming physical quantities in the local into the quantities in the universal coordinates or its reverse transformation, but defining end forces which are independent each other in the element coordinates. Since the element end deformations are the counterparts of the forces, the deformations become geometrically clear. The concept of the end deformations and the end forces is common with the method of slope deflection in elemental statics. Kassimali; Abbasnia (1991) which developed Oran (1973) used the member orientation matrix and the joint orientation matrix. Those matrices are the same concept as the element coordinates and the element end coordinates in the paper. However, the paper has several differences from Kassimali; Abbasnia (1991). The end rotations regarding bending and torsion of the element should be axial vectors in the consistent/exact compatibility and the convergence criterion should not use the increment displacement but the unbalanced forces at nodes.

The paper follows the basic concept shown in Goto (1983). Iguchi; Goto; Ijima; Obiya (2003) have already certified the theory by the experiment of folding an arch by torsion. The paper particularly details the element coordinates, the element end deformations based on the energy principle, and deriving the deformations of a beam element in space with geometric strictness.

2 Concept of the Theory

2.1 Equilibrium equation

The total potential energy of a structure that consists of finite elements is,

$$\Pi = \sum_e V_e - W \tag{1}$$

where W is the potential of the nodal force, **U,** and V_e is the strain energy in the element, e.

[1] Saga University, Saga, Japan
[2] Forum 8 Co., Ltd., Miyazaki, Japan

From energy principles,

$$\frac{\partial \Pi}{\partial \mathbf{u}} = \sum_e \frac{\partial V_e}{\partial \mathbf{u}} - \mathbf{U} = \mathbf{0} \tag{2}$$

where $\mathbf{u}$ is the nodal displacement.

FEM directly solves Eq. 2 from V_e through the displacement functions expressed by the nodal displacement. However, it is quite difficult to obtain the functions by exactly treating finite rotation with geometric strictness. On the other hand, though the method of slope deflection is the same displacement method as FEM, the method treats deformation of the element as behavior of a simple beam. If the element has such support condition, the total potential energy can be defined in the element and the support condition. We call the system the element coordinates.

$$\Pi_e = V_e - W_e \tag{3}$$

where W_e is the work of the element end forces, $\mathbf{S}_e$. When the element is a beam, the total number of the element end forces is twelve. The twelve forces must be naturally equilibrium. The reaction forces in the support condition of the simple beam are six in the twelve forces. In Eq. 3, the work of the reaction forces vanishes in rigid body displacement. The remainders of the six forces give the beam deformation as the external forces in the element coordinate. Hence $\mathbf{S}_e$ consists of the end forces. The end forces are conservative and independent each other.

In the element coordinates, the energy principle gives,

$$\frac{\partial \Pi_e}{\partial \mathbf{s}_e} = \frac{\partial V_e}{\partial \mathbf{s}_e} - \mathbf{S}_e = \mathbf{0} \tag{4}$$

where $\mathbf{s}_e$ is the element end deformations. Since the deformations and the element end forces are counterparts each other, the deformations become geometrically clear and are restricted at the element ends. For example, when one of the end forces is a moment, the counterpart is a rotation as an axial vector given at the element end. The work of the moment is a scalar product between the moment vector and the rotation vector.

In applying Eq. 4 to each element, the element end deformation keeps continuity by defining the element end coordinates. The end coordinates rotate with following the rotation of the node connected to the element end. Hence all of the element ends fixed to the node identically rotate.

From Eq. 4, the differential of the strain energy in the element, e, in Eq. 2 becomes,

$$\frac{\partial V_e}{\partial \mathbf{u}} = \frac{\partial \mathbf{s}_e^T}{\partial \mathbf{u}} \frac{\partial V_e}{\partial \mathbf{s}_e} = \frac{\partial \mathbf{s}_e^T}{\partial \mathbf{u}} \mathbf{S}_e \tag{5}$$

The differential of the element end deformation functions as deriving the all of the element end forces from the end forces independent each other as well as transforming the element end forces into the components in the universal coordinates.

Substituting Eq. 5 into Eq. 2, the equilibrium equation at the nodes in the structure is,

$$\mathbf{U} - \sum_e \frac{\partial \mathbf{s}_e^T}{\partial \mathbf{u}} \mathbf{S}_e = \mathbf{0} \tag{6}$$

The method solves Eq. 6. Since the element end deformations are geometrically clear, the accuracy of the method depends on the element end forces derived from Eq. 4. Namely, more exact expression of Eq. 4 results in equilibrium solutions more identical to real phenomena.

Eq. 6 is a general expression without restricting its application to beam element. For example, if Eq. 6 is applied to a plate element, the element end forces are defined by statically determinative support conditions. When the shape function in FEM is not expressed by the nodal displacement but the element end deformation, the element stiffness equation is easily obtained as the relation between the end forces and the end deformations.

If FEM is defined as using shape functions and making the average residual zero, the demerit is short of geometric strictness due to shape functions expressed by nodal displacement. However, if the shape functions are expressed by the element end deformation, the various functions already developed in FEM are available for getting element stiffness equations.

2.2 Tangent stiffness equation

In order to solve Eq. 6, the method needs the tangent stiffness equation as well as FEM.

From the equilibrium of Eq. 6, the infinitesimal increment of the nodal force is,

$$\delta \mathbf{U} = \sum_e \frac{\partial \mathbf{s}_e^T}{\partial \mathbf{u}} \delta \mathbf{S}_e + \sum_e \delta \left(\frac{\partial \mathbf{s}_e^T}{\partial \mathbf{u}} \right) \mathbf{S}_e \tag{7}$$

The first term expresses the increment of the element end forces, and the second term is direction changes of the end forces.

The infinitesimal increment of the end forces is obtained from the tangent equation of the element end force equation. Since this section conceptually explains the theory, a concrete equation of the element end force of beam is shown in Section 5. The tangent equation of the equation is defined as,

$$\delta \mathbf{S}_e = \mathbf{k}_e \delta \mathbf{s}_e \tag{8}$$

The infinitesimal increment of the element end deformation is,

$$\delta \mathbf{s}_e \frac{\partial \mathbf{s}_e}{\partial \mathbf{u}^T} \delta \mathbf{u} \tag{9}$$

Since the element end forces are constant in the second term in Eq. 7, the term becomes,

$$\delta \left(\frac{\partial \mathbf{s}_e^T}{\partial \mathbf{u}} \right) \mathbf{S}_e = \frac{\partial}{\partial \mathbf{u}} \left(\mathbf{s}_e^T \mathbf{S}_e \right) \frac{\partial}{\partial \mathbf{u}^T} \delta \mathbf{u} \tag{10}$$

Substituting Eq. 8, 9 and 10 into Eq. 7, the tangent stiffness equation is,

$$\begin{aligned} \delta \mathbf{U} &= \sum_e \left\{ \frac{\partial \mathbf{s}_e^T}{\partial \mathbf{u}} \mathbf{k}_e \frac{\partial \mathbf{s}_e}{\partial \mathbf{u}^T} + \frac{\partial}{\partial \mathbf{u}} \left(\mathbf{s}_e^T \mathbf{S}_e \right) \frac{\partial}{\partial \mathbf{u}^T} \right\} \delta \mathbf{u} \\ &= \left(\mathbf{K}_O + \mathbf{K}_G \right) \delta \mathbf{u} \end{aligned} \tag{11}$$

where

$$\mathbf{K}_O \equiv \frac{\partial \mathbf{s}_e^T}{\partial \mathbf{u}} \mathbf{k}_e \frac{\mathbf{s}_e}{\partial \mathbf{u}^T} \tag{12}$$

$$\mathbf{K}_G \equiv \frac{\partial}{\partial \mathbf{u}} \left(\mathbf{s}_e^T \mathbf{S}_e \right) \frac{\partial}{\partial \mathbf{u}^T} \tag{13}$$

Eq. 12 is due to the element stiffness itself, and Eq. 13 is the geometric stiffness due to changing the directions of the end forces.

3 Element End Deformation of a Beam

The element end deformation of beam can be exactly obtained by simple knowledge of finite rotation.

A beam element in space has twelve degrees of freedom and the six equations of equilibrium. Six forces in the twelve forces at both ends are independent each other. Therefore, there are various combinations of the element end forces selected from the twelve forces.

A set of the element end forces shown in Fig. 1 has the support condition similar to a simple beam. The element coordinates is rational in terms of reducing geometrically nonlinear effect in the element and in terms of equality between both ends. For example, a cantilever can be also selected as one of statically determinate element coordinates. However, it is clear that the end deformation defined in the cantilever is larger than a simple beam. Besides, since it is impossible to express completely non-

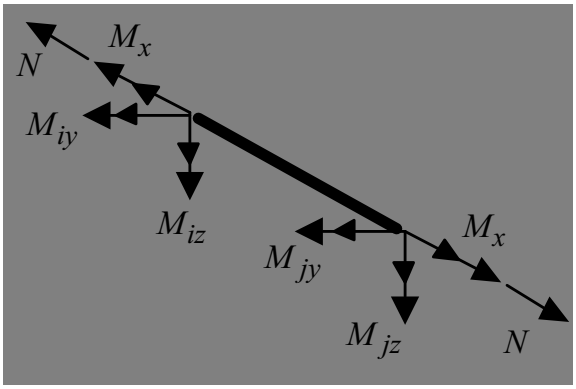

Figure 1 : Element coordinates and element end coordinates

linear phenomena in the element coordinates, correspondence of the fixed or free end in the cantilever coordinates to the node affects equilibrium solution of a structure.

On the other hand, both ends of the simple beam have equal conditions.

From the counterparts of the element end forces in Fig. 1, a set of the element end deformations becomes the elongation, Δl, and the components of the rotation vectors at both ends i and j, $\theta_x, \theta_{iy}, \theta_{iz}, \theta_{jy}, \theta_{jz}$. The two end coordinates shown in Fig. 2 move and rotate along the nodal displacement. When the element coordinates rotates and agrees with one side of the end coordinates, the given rotation is the end deformation regarding torsion and bending. Analytically, however, finding the element coordinates from both end coordinates after nodal displacement derives the end deformation.

Expressing the nodal rotations, $\Delta \mathbf{x}_i, \Delta \mathbf{x}_j$, by its angle and its direction,

$$\Delta \mathbf{x}_i = \theta_i^p \mathbf{e}_i^p, \tag{14}$$

$$\Delta \mathbf{x}_j = \theta_j^p \mathbf{e}_j^p \tag{15}$$

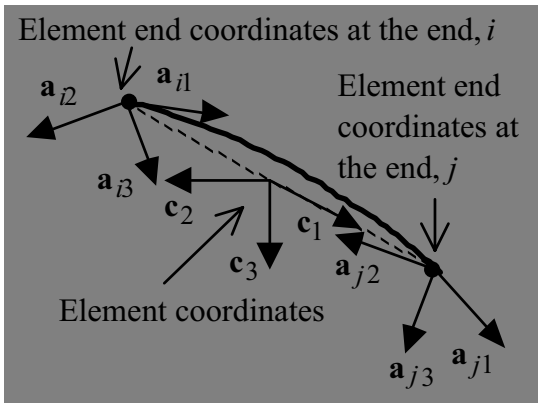

Figure 2 : Element end forces

When the unit vectors parallel to the axes in both end coordinates are $\mathbf{a}^p_{i1}, \mathbf{a}^p_{i2}, \mathbf{a}^p_{i3}$ at the end, i, and $\mathbf{a}^p_{j1}, \mathbf{a}^p_{j2}, \mathbf{a}^p_{j3}$ at the end, j, these axes after the finite rotation of the node becomes the following vectors. As an example, the first axis $\mathbf{a}^p_{i1}$, changes into $\mathbf{a}_{i1}$.

$$\mathbf{a}_{i1} = \mathbf{e}_i^{p^T}\mathbf{a}^p_{i1}(1-\cos\theta^p_i)\mathbf{e}^p_i + \cos\theta^p_i\mathbf{a}^p_{i1} + \sin\theta^p_i\mathbf{e}^p_i \times \mathbf{a}^p_{i1} \tag{16}$$

The previous end coordinates in Eq. 16 include the previous deformation. Kassimali; Abbasnia (1991) obtained the end coordinates from the finite rotation of the element coordinates before the nodal displacement. This means computing the increment deformation of the element and adding it to the previous deformation gives the total deformation. Even if the increment rotation is very small, however, the sum makes accumulative error. Hence, considering the finite rotation in the element deformation, the total end rotation has to be computed [Iguchi, S; Goto, S; Ijima, K; Obiya, H (1997)].

The procedure to obtain the element coordinates from both end coordinates is the following. By the first rotation, each first axis in both coordinates is made to coincide with the line which connects both ends. The second rotation fits the second axes at both ends each other. The coordinates after the two rotations is the element coordinates. The rotation vector composed by the two rotations gives the element end deformation.

When the first rotation vectors at both ends are $\theta_{i1}\mathbf{e}_{i1}$, $\theta_{j1}\mathbf{e}_{j1}$, the angles and the directions are obtained by the following equations.

$$\cos\theta_{i1} = \mathbf{a}^T_{i1}\mathbf{c}_1 \tag{17}$$

$$\mathbf{e}_{i1}\sin\theta_{i1} = \mathbf{a}_{i1} \times \mathbf{c}_1 \tag{18}$$

where $\mathbf{c}_1$ is the unit vector parallel to the line that connects both ends.

The locus of the first axis during the rotation makes a plane, and $\mathbf{e}_{i1}$ is orthogonal to $\mathbf{c}_1$.

The unit vectors of the second axis and the third one after the first rotation at the end i are,

$$\mathbf{b}_{i2} = \mathbf{a}_{i2} - \frac{\mathbf{c}_1^T\mathbf{a}_{i2}}{1+\mathbf{c}_1^T\mathbf{a}_{i1}}(\mathbf{c}_1+\mathbf{a}_{i1}) \tag{19}$$

$$\mathbf{b}_{i3} = \mathbf{a}_{i3} - \frac{\mathbf{c}_1^T\mathbf{a}_{i3}}{1+\mathbf{c}_1^T\mathbf{a}_{i1}}(\mathbf{c}_1+\mathbf{a}_{i1}) \tag{20}$$

The vectors at the end, j, are obtained by changing the suffix, i, to j in Eq. 17 to 20.

After the first rotation, the open angle, θ_{ij}, between the second axes at both ends is,

$$\cos\theta_{ij} = \mathbf{b}^T_{i2}\mathbf{b}_{j2} \tag{21}$$

$$\mathbf{c}_1\sin\theta_{ij} = \mathbf{b}_{i2} \times \mathbf{b}_{j2} \tag{22}$$

When the angles of the second rotation are

θ_{i2} and θ_{j2}, $\theta_{i2}\mathbf{c}_1$ and $\theta_{j2}\mathbf{c}_1$ are the second rotation vectors, where $\theta_{i2}-\theta_{j2}=\theta_{ij}$. The angles are described later in detail.

There are some methods to obtain the vector composed by the first rotation vector and the second one. Using Hamilton's quaternion, the composition becomes simple.

When the vector, $\mathbf{a}$, changes to $\mathbf{b}$ by the rotation, $\theta\mathbf{e}_r$, using the quaternion,

$$\mathbf{b} = \left(\cos\frac{\theta}{2},\ \mathbf{e}_r\sin\frac{\theta}{2}\right) \otimes (0,\mathbf{a}) \otimes \left(\cos\frac{\theta}{2},\ -\mathbf{e}_r\sin\frac{\theta}{2}\right) \tag{23}$$

Multiplication by the operator $\otimes$ is usual between a scalar and a vector or between two scalars. The product between two vectors complies with the following definition. When $\mathbf{e}_1$, $\mathbf{e}_2$ and $\mathbf{e}_3$ are the unit vectors parallel to the axes in the orthogonal coordinates,

$$\left.\begin{array}{l} \mathbf{e}_1\otimes\mathbf{e}_1 = \mathbf{e}_2\otimes\mathbf{e}_2 = \mathbf{e}_3\otimes\mathbf{e}_3 = -1 \\ \mathbf{e}_1\otimes\mathbf{e}_2 = -\mathbf{e}_2\otimes\mathbf{e}_1 = \mathbf{e}_3 \\ \mathbf{e}_2\otimes\mathbf{e}_3 = -\mathbf{e}_3\otimes\mathbf{e}_2 = \mathbf{e}_1 \\ \mathbf{e}_3\otimes\mathbf{e}_1 = -\mathbf{e}_1\otimes\mathbf{e}_3 = \mathbf{e}_2 \end{array}\right\} \tag{24}$$

Complying with Eq. 24, Eq. 23 becomes a similar equation to Eq. 16.

When $\theta_{ic}\mathbf{e}_{ic}$ and $\theta_{jc}\mathbf{e}_{jc}$ are the rotation vector composed by the two rotation, the rotation vector, $\theta_{ic}\mathbf{e}_{ic}$, is reverse to the composition of the first rotation, $\theta_{i1}\mathbf{e}_{i1}$, and the second, $\theta_{i2}\mathbf{c}_1$. Hence, using the quaternion,

$$\left(\cos\frac{\theta_{ic}}{2}, \mathbf{e}_{ic}\sin\frac{\theta_{ic}}{2}\right) = \left(\cos\frac{\theta_{i1}}{2}, -\mathbf{e}_{i1}\sin\frac{\theta_{i1}}{2}\right) \otimes \left(\cos\frac{\theta_{i2}}{2}, -\mathbf{c}_1\sin\frac{\theta_{i2}}{2}\right) \quad (25)$$

Applying Eq. 24 to Eq. 25,

$$\cos\frac{\theta_{ic}}{2} = \cos\frac{\theta_{i1}}{2}\cos\frac{\theta_{i2}}{2} \quad (26)$$

$$\mathbf{e}_{ic}\sin\frac{\theta_{ic}}{2} = \sin\frac{\theta_{i1}}{2}\cos\frac{\theta_{i2}}{2}\mathbf{e}_{i1} - \cos\frac{\theta_{i1}}{2}\sin\frac{\theta_{i2}}{2}\mathbf{c}_1 + \sin\frac{\theta_{i1}}{2}\sin\frac{\theta_{i2}}{2}\mathbf{e}_{i1}\times\mathbf{c}_1 \quad (27)$$

The composed rotation vector at the end j is also obtained in the same way.

In Eq. 26 and 27, the angles of the second rotation are unknown. If the angles are half of the open angle between the second axes at both ends after the first rotation, the angles are,

$$\theta_{i2} = \frac{\theta_{ij}}{2},\ \theta_{j2} = -\frac{\theta_{ij}}{2} \quad (28)$$

However, Eq. 28 does not equalize the first components of the composed vectors at both ends. In order to keep the equality, the second rotation must fulfill the following equation.

$$\left(\theta_{ic}\mathbf{e}_{ic} + \theta_{jc}\mathbf{e}_{jc}\right)^T\mathbf{c}_1 = 0 \quad (29)$$

Though Eq. 29 is strict, the equation does not explicitly give the second rotation angle. Hence, a kind of iteration is needed to solve Eq. 29. As a result of computational comparison between Eq. 28 and 29, the solution using Eq. 28 has enough accuracy.

After determining the angle of the second rotation, the directions of the second axis, $\mathbf{c}_2$, and the third axis, $\mathbf{c}_3$, in the element coordinates are,

$$\mathbf{c}_2 = \mathbf{b}_{i2}\cos\frac{\theta_{i2}}{2} + \mathbf{b}_{i3}\sin\frac{\theta_{i2}}{2} \quad (30)$$

$$\mathbf{c}_3 = -\mathbf{b}_{i2}\sin\frac{\theta_{i2}}{2} + \mathbf{b}_{i3}\cos\frac{\theta_{i2}}{2} \quad (31)$$

From the rotation vectors at both ends and the element coordinates, the components of the rotations are,

$$\theta_x = \left(\theta_{jc}\mathbf{e}_{jc} - \theta_{ic}\mathbf{e}_{ic}\right)^T\mathbf{c}_1 \quad (32)$$

$$\theta_{iy} = \theta_{ic}\mathbf{e}_{ic}^T\mathbf{c}_2 \quad (33)$$

$$\theta_{iz} = \theta_{ic}\mathbf{e}_{ic}^T\mathbf{c}_3 \quad (34)$$

$$\theta_{jy} = \theta_{jc}\mathbf{e}_{jc}^T\mathbf{c}_2 \quad (35)$$

$$\theta_{jz} = \theta_{jc}\mathbf{e}_{jc}^T\mathbf{c}_3 \quad (36)$$

In this manner, restricting the element deformations at the ends, the deformations are expressed with geometrical strictness and without any approximation.

After the nodal displacement is given, the procedure up to getting the unbalanced forces is the following. Computing the elongation from the distance between both ends and the element end deformation by Eqs. 32 to 36, then computing the element end forces by using the equations in Section 5, then the end forces and the external forces are summed up by Eq. 6. The resultants are the unbalanced forces.

4 Geometric Stiffness Matrix of a Beam

The geometric stiffness is due to changing the directions of element end forces by the infinitesimal nodal displacement from equilibrium. Therefore, the equilibrium position is a reference and the geometric stiffness is,

$$\mathbf{K}_G = \sum_e \frac{\partial}{\partial\delta\mathbf{u}}\left(\delta W_e\right)\frac{\partial}{\partial\delta\mathbf{u}^T} \quad (37)$$

where $\delta\mathbf{u} = \left\{\delta\mathbf{u}_i^T\ \delta\mathbf{x}_i^T\ \delta\mathbf{u}_j^T\ \delta\mathbf{x}_j^T\right\}$ is the infinitesimal displacement, $\delta\mathbf{u}_i$ and $\delta\mathbf{u}_j$ are the translations at both ends, and $\delta\mathbf{x}_i$ and $\delta\mathbf{x}_j$ are the rotations.

δW_e is the work of the constant end forces in the present equilibrium, as follows,

$$\delta W_e = N\delta l + M_x\delta\theta_x + M_{iy}\delta\theta_{iy} + M_{iz}\delta\theta_{iz} + M_{jy}\delta\theta_{jy} + M_{jz}\delta\theta_{jz} \quad (38)$$

where $\delta l, \delta\theta_x, \delta\theta_{iy}, \delta\theta_{iz}, \delta\theta_{jy}, \delta\theta_{jz}$ are the infinitesimal increments of the element end deformations.

Expressing the increments by the second order of the infinitesimal displacement, the geometrical stiffness is obtained from Eq. 37. When $\mathbf{c}_1$, $\mathbf{c}_2$ and $\mathbf{c}_3$ are the directions

of the element coordinate axes, the deformations in the second order are expressed by,

$$\delta l = \mathbf{c}_1^T \delta \mathbf{u}_{ji} + \frac{1}{2l}\left\{ \delta \mathbf{u}_{ji}^T \delta \mathbf{u}_{ji} - \left(\mathbf{c}_1^T \delta \mathbf{u}_{ji} \right)^2 \right\} \tag{39}$$

$$\delta\theta_x = \mathbf{c}_1^T \delta \mathbf{x}_{ji} + \frac{1}{2}\mathbf{c}_2^T \delta \mathbf{x}_{ji} \mathbf{c}_2^T \delta \overline{\mathbf{u}}_{ji} + \frac{1}{2}\mathbf{c}_3^T \delta \mathbf{x}_{ji} \mathbf{c}_3^T \delta \overline{\mathbf{u}}_{ji} \tag{40}$$

$$\begin{aligned}\delta\theta_{iy} = {} & \mathbf{c}_2^T \delta \mathbf{x}_i + \mathbf{c}_3^T \delta \overline{\mathbf{u}}_{ji} - \mathbf{c}_1^T \delta \overline{\mathbf{u}}_{ji} \mathbf{c}_3^T \delta \overline{\mathbf{u}}_{ji} \\ & + \frac{1}{4}\mathbf{c}_1^T \delta \mathbf{x}_i \left(\mathbf{c}_3^T \delta \mathbf{x}_i - 3\mathbf{c}_2^T \delta \overline{\mathbf{u}}_{ji} \right) \\ & + \frac{1}{4}\mathbf{c}_1^T \delta \mathbf{x}_j \left(\mathbf{c}_3^T \delta \mathbf{x}_i - \mathbf{c}_2^T \delta \overline{\mathbf{u}}_{ji} \right)\end{aligned} \tag{41}$$

$$\begin{aligned}\delta\theta_{iz} = {} & \mathbf{c}_3^T \delta \mathbf{x}_i - \mathbf{c}_2^T \delta \overline{\mathbf{u}}_{ji} + \mathbf{c}_1^T \delta \overline{\mathbf{u}}_{ji} \mathbf{c}_2^T \delta \overline{\mathbf{u}}_{ji} \\ & - \frac{1}{4}\mathbf{c}_1^T \delta \mathbf{x}_i \left(\mathbf{c}_2^T \delta \mathbf{x}_i + 3\mathbf{c}_3^T \delta \overline{\mathbf{u}}_{ji} \right) \\ & - \frac{1}{4}\mathbf{c}_1^T \delta \mathbf{x}_j \left(\mathbf{c}_2^T \delta \mathbf{x}_i + \mathbf{c}_3^T \delta \overline{\mathbf{u}}_{ji} \right)\end{aligned} \tag{42}$$

$$\begin{aligned}\delta\theta_{jy} = {} & \mathbf{c}_2^T \delta \mathbf{x}_j + \mathbf{c}_3^T \delta \overline{\mathbf{u}}_{ji} - \mathbf{c}_1^T \delta \overline{\mathbf{u}}_{ji} \mathbf{c}_3^T \delta \overline{\mathbf{u}}_{ji} \\ & + \frac{1}{4}\mathbf{c}_1^T \delta \mathbf{x}_j \left(\mathbf{c}_3^T \delta \mathbf{x}_j - 3\mathbf{c}_2^T \delta \overline{\mathbf{u}}_{ji} \right) \\ & + \frac{1}{4}\mathbf{c}_1^T \delta \mathbf{x}_i \left(\mathbf{c}_3^T \delta \mathbf{x}_j - \mathbf{c}_2^T \delta \overline{\mathbf{u}}_{ji} \right)\end{aligned} \tag{43}$$

$$\begin{aligned}\delta\theta_{jz} = {} & \mathbf{c}_3^T \delta \mathbf{x}_j - \mathbf{c}_2^T \delta \overline{\mathbf{u}}_{ji} + \mathbf{c}_1^T \delta \overline{\mathbf{u}}_{ji} \mathbf{c}_2^T \delta \overline{\mathbf{u}}_{ji} \\ & - \frac{1}{4}\mathbf{c}_1^T \delta \mathbf{x}_j \left(\mathbf{c}_2^T \delta \mathbf{x}_j + 3\mathbf{c}_3^T \delta \overline{\mathbf{u}}_{ji} \right) \\ & - \frac{1}{4}\mathbf{c}_1^T \delta \mathbf{x}_i \left(\mathbf{c}_2^T \delta \mathbf{x}_j + \mathbf{c}_3^T \delta \overline{\mathbf{u}}_{ji} \right)\end{aligned} \tag{44}$$

where l is the distance between both ends and,

$$\delta \mathbf{u}_{ji} = \delta \mathbf{u}_j - \delta \mathbf{u}_i, \tag{45}$$

$$\delta \overline{\mathbf{u}}_{ji} = \delta \mathbf{u}_{ji} / l \tag{46}$$

$$\delta \mathbf{x}_{ji} = \delta \mathbf{x}_j - \delta \mathbf{x}_i \tag{47}$$

From the differential in Eq. 37, the geometric stiffness becomes,

$$\begin{Bmatrix} \delta \mathbf{U}_i \\ \delta \mathbf{X}_i \\ \delta \mathbf{U}_j \\ \delta \mathbf{X}_j \end{Bmatrix} = \begin{bmatrix} \mathbf{k}_{11} & \mathbf{k}_{12} & -\mathbf{k}_{11} & \mathbf{k}_{14} \\ & \mathbf{k}_{22} & -\mathbf{k}_{12}^T & \mathbf{k}_{24} \\ & & \mathbf{k}_{11} & -\mathbf{k}_{14} \\ sym. & & & \mathbf{k}_{44} \end{bmatrix} \begin{Bmatrix} \delta \mathbf{u}_i \\ \delta \mathbf{x}_i \\ \delta \mathbf{u}_j \\ \delta \mathbf{x}_j \end{Bmatrix} \tag{48}$$

where

$$\mathbf{k}_{11} = \frac{N}{l}\left(\mathbf{I} - \mathbf{c}_1 \mathbf{c}_1^T \right) - \frac{M_{iy} + M_{jy}}{l^2}\left(\mathbf{c}_1 \mathbf{c}_3^T + \mathbf{c}_3 \mathbf{c}_1^T \right) + \frac{M_{iz} + M_{jz}}{l^2}\left(\mathbf{c}_1 \mathbf{c}_2^T + \mathbf{c}_2 \mathbf{c}_1^T \right) \tag{49}$$

$$\mathbf{k}_{12} = \frac{M_x}{2l}\left(\mathbf{I} - \mathbf{c}_1 \mathbf{c}_1^T \right) + \frac{3M_{iy} + M_{jy}}{4l}\mathbf{c}_2 \mathbf{c}_1^T + \frac{3M_{iz} + M_{jz}}{4l}\mathbf{c}_3 \mathbf{c}_1^T \tag{50}$$

$$\mathbf{k}_{14} = -\frac{M_x}{2l}\left(\mathbf{I} - \mathbf{c}_1 \mathbf{c}_1^T \right) + \frac{M_{iy} + 3M_{jy}}{4l}\mathbf{c}_2 \mathbf{c}_1^T + \frac{M_{iz} + 3M_{jz}}{4l}\mathbf{c}_3 \mathbf{c}_1^T \tag{51}$$

$$\mathbf{k}_{22} = \frac{M_{iy}}{4}\left(\mathbf{c}_1 \mathbf{c}_3^T + \mathbf{c}_3 \mathbf{c}_1^T \right) - \frac{M_{iz}}{4}\left(\mathbf{c}_1 \mathbf{c}_2^T + \mathbf{c}_2 \mathbf{c}_1^T \right) \tag{52}$$

$$\mathbf{K}_{24} = \frac{M_{iy}}{4}\mathbf{c}_3 \mathbf{c}_1^T + \frac{M_{iz}}{4}\mathbf{c}_1 \mathbf{c}_3^T - \frac{M_{iz}}{4}\mathbf{c}_2 \mathbf{c}_1^T - \frac{M_{jz}}{4}\mathbf{c}_1 \mathbf{c}_2^T \tag{53}$$

$$\mathbf{k}_{44} = \frac{M_{jy}}{4}\left(\mathbf{c}_1 \mathbf{c}_3^T + \mathbf{c}_3 \mathbf{c}_1^T \right) - \frac{M_{jz}}{4}\left(\mathbf{c}_1 \mathbf{c}_2^T + \mathbf{c}_2 \mathbf{c}_1^T \right) \tag{54}$$

where **I** is the unit matrix of 3x3.

5 Element End Force Equation

Since the element end deformations in the method do not include any approximation, difference between the analysis and a real phenomenon results from the accuracy of the relation between the end deformations and the end forces in the element.

Effects of a non-stress shape of an element appear in the element end force equations. It is unnecessary to modify the element end deformations and the geometric stiffness in response to the non-stress shape of the element. Similarly, if considering inelastic characteristic of the element and geometric strictness in the element, these are also condensed into the end force equations.

In the computational example, assuming that the elements are straight in non-stress, the following relation well known as the beam-column theory is used,

$$N = \frac{EA}{l_o}\Delta l \tag{55}$$

$$M_x = \frac{GJ}{l_0}\theta_x \tag{56}$$

$$\begin{Bmatrix} M_{im} \\ M_{jm} \end{Bmatrix} = \frac{EI_m}{l_0}\begin{bmatrix} a_m & b_m \\ b_m & a_m \end{bmatrix}\begin{Bmatrix} \theta_{im} \\ \theta_{jm} \end{Bmatrix} \tag{57}$$

where m is y or z, l_0 is the non-stress length of the element. Using the beam-column theory, the element end

force, N, becomes equivalent to the axial force. When the axial force is tension, $N > 0$,

$$a_m = \frac{\omega_m^2 \cosh\omega_m - \omega_m \sinh\omega_m}{\omega_m \sinh\omega_m + 2(1-\cosh\omega_m)} \tag{58a}$$

$$b_m \frac{\omega_m \sinh\omega_m - \omega_m^2}{\omega_m \sinh\omega_m + 2(1-\cosh\omega_m)} \tag{58b}$$

where $\omega_m = \sqrt{|N|/(EI_m)}$. When the axial force is compression, $N < 0$,

$$a_m = \frac{\omega_m^2 \cos\omega_m - \omega_m \sin\omega_m}{\omega_m \sin\omega_m - 2(1-\cos\omega_m)} \tag{59a}$$

$$b_m = \frac{\omega_m \sin\omega_m - \omega_m^2}{\omega_m \sin\omega_m - 2(1-\cos\omega_m)} \tag{59b}$$

When the axial force is near zero, instead of Eq. 58 or 59, the following series of $\lambda_m = Nl_0^2/(EI_m)$ is used,

$$a_m = 4 + \frac{2}{15}\lambda_m - \frac{11}{6300}\lambda_m^2 + \frac{1}{27000}\lambda_m^3 \tag{60a}$$

$$b_m = 2 - \frac{1}{30}\lambda + \frac{13}{12600}\lambda_m^2 - \frac{11}{378000}\lambda_m^3 \tag{60b}$$

In the equations, the element is elastic and the geometric nonlinearity in the element is neglected.

When obtaining the tangent stiffness matrix related to the element stiffness, Eq. 12, though Eq. 57 includes the axial force, the stiffness matrix, $\mathbf{k}_e$, consists of the element end force equations, 55, 56 and 57. This is because the elongation and the rotational components are independent each other in the assumed model of the element.

The differential of the element end deformations in Eq. 6 or Eq. 12 is obtained by using the first order in Eqs. 39 to 44.

$$\begin{Bmatrix} \mathbf{U}_i \\ \mathbf{X}_i \\ \mathbf{U}_j \\ \mathbf{X}_j \end{Bmatrix} = \begin{bmatrix} -\mathbf{c}_1 & \mathbf{0} & -\frac{\mathbf{c}_3}{l} & -\frac{\mathbf{c}_3}{l} & \frac{\mathbf{c}_2}{l} & \frac{\mathbf{c}_2}{l} \\ \mathbf{0} & -\mathbf{c}_1 & \mathbf{c}_2 & \mathbf{0} & \mathbf{c}_3 & \mathbf{0} \\ \mathbf{c}_1 & \mathbf{0} & \frac{\mathbf{c}_3}{l} & \frac{\mathbf{c}_3}{l} & -\frac{\mathbf{c}_2}{l} & -\frac{\mathbf{c}_2}{l} \\ \mathbf{0} & \mathbf{c}_1 & \mathbf{0} & \mathbf{c}_2 & \mathbf{0} & \mathbf{c}_3 \end{bmatrix} \begin{Bmatrix} N \\ M_x \\ M_{iy} \\ M_{jy} \\ M_{iz} \\ M_{jz} \end{Bmatrix} \tag{61}$$

Furthermore, Eq. 61 is the same as the equation that is derived from transforming the element end forces, which include the reaction forces in the element coordinates, into the components in the universal coordinates.

6 Computational Example

Rotating an end around the tangent axis in a ring with a slit, the ring is folded into the double circles by 2π radians of rotation. As a computational example, the folding process of the ring was simulated by the method.

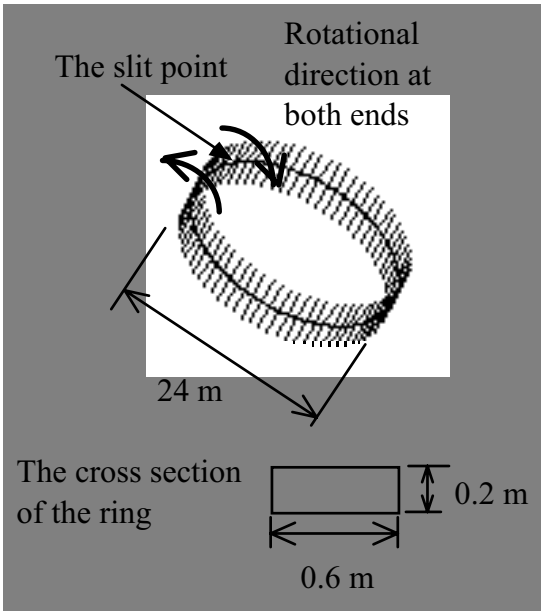

Figure 3 : Polygonal ring composed by 72 elements

Fig. 3 shows the ring used for the computation. The Young's modulus of the element is 205800 MPa. The straight elements of 72 compose the ring. Hence the ring is a regular polygon as a primary shape. The computation uses also the rings composed by 18 elements and 36 elements.

Both ends of the ring at the slit rotate with the same angle in the opposite direction each other around the tangent axis at the slit.

The rigid lines attached to the nodes of the are normal to the plane in the primary form, and rotate along with the nodes.

Fig 4 shows the folding process. The angles in the figure are the total angle given both ends. When completing the double circles, the rigid lines fit in each other. If treating the increment rotation in the element as a polar vector without using finite rotation, the rigid lines do not fit like Fig. 4.

Fig. 5 shows the convergent process of the maximum unbalanced forces in the nodes of the ring composed by

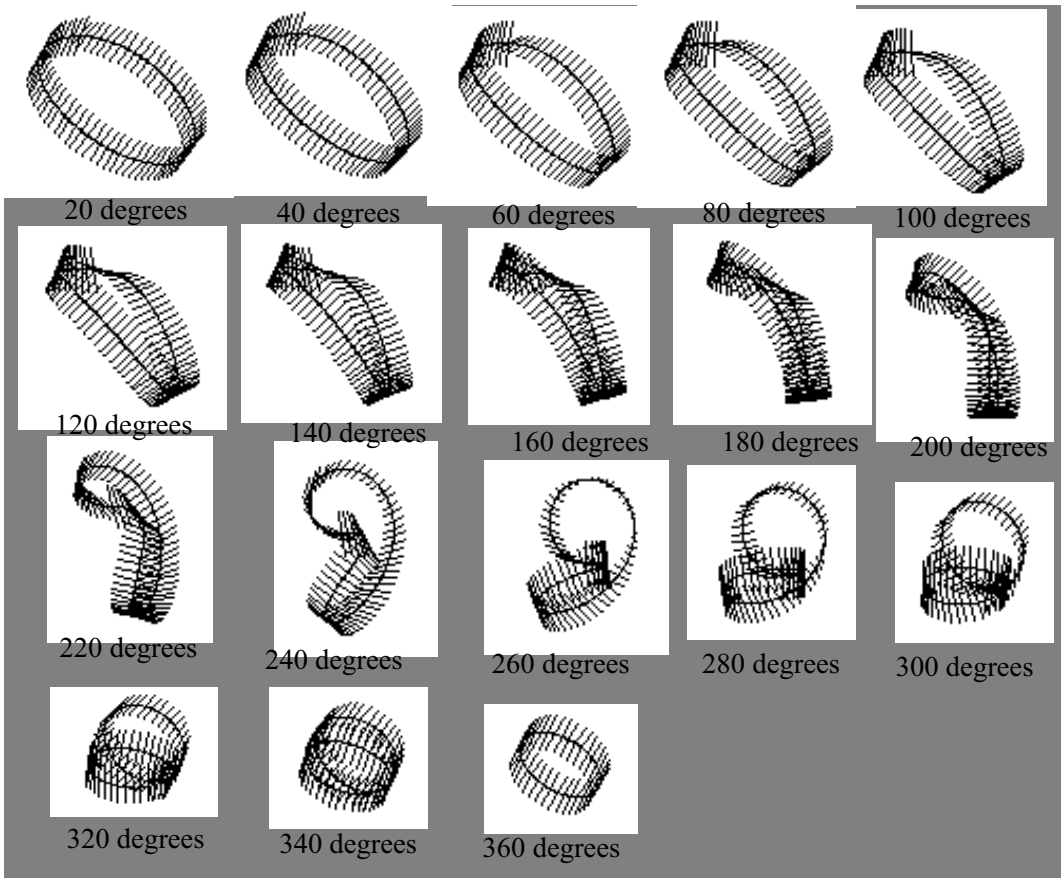

Figure 4 : Folding process of the polygonal ring with slit

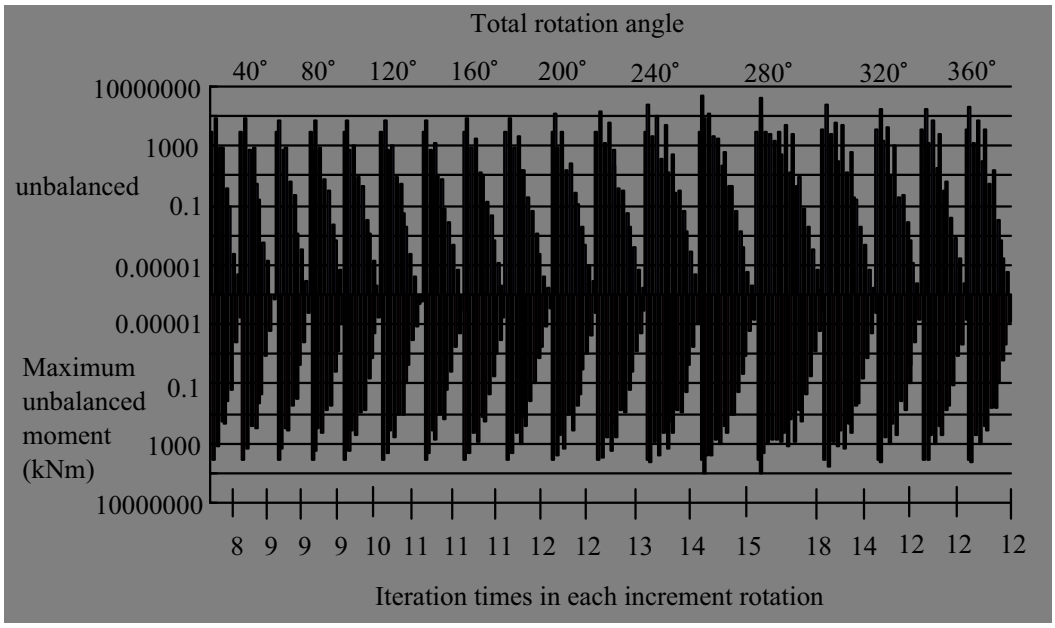

Figure 5 : Covergent process of the maximum unbalanced force in the ring of 18 elements

18 elements. In the cases of the rings of 18 and 36 elements, even if using the increment rotation of 20 degrees given both ends, the folding process can be completed. The ring of 72 elements needs to reduce the increment rotation to 10 degrees.

The buckling analysis may verify the accuracy of the tangent stiffness matrix [Hsiao; Lin, (2003)]. However, since the matrix in the method includes the six element end forces, it is difficult to obtain a theoretical solution that can verify all of the coefficients in the matrix. Therefore, though not sufficiently prove Eq. 48 to be strict, the convergent process of the maximum unbalanced forces is shown in Fig.5. The unbalanced forces converge in less than the allowable value given by considering the significant figure in the computation.

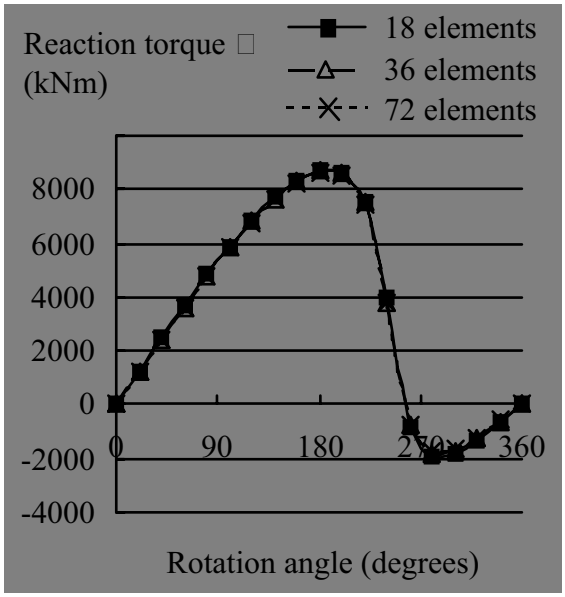

Figure 6 : Reaction torque at an end

Fig. 6 is the relation between the rotation angle and the reaction torque at an end and Figs. 7 and 8 are the end forces of the middle element in the ring. When completing folding the ring, the reaction torque, the axial force and the end moments, M_x and M_z, become nearly zero regardless of the number of dividing the ring. In the theoretical solution, the forces must be zero. Hence even if using small number of elements composing the ring, the solution has sufficient accuracy.

The effect of dividing appears only in the end moment, M_z, on the way of folding. Since presuming the end moment, M_z, to be very small, a ring model of 100 elements is enough to simulate the folding.

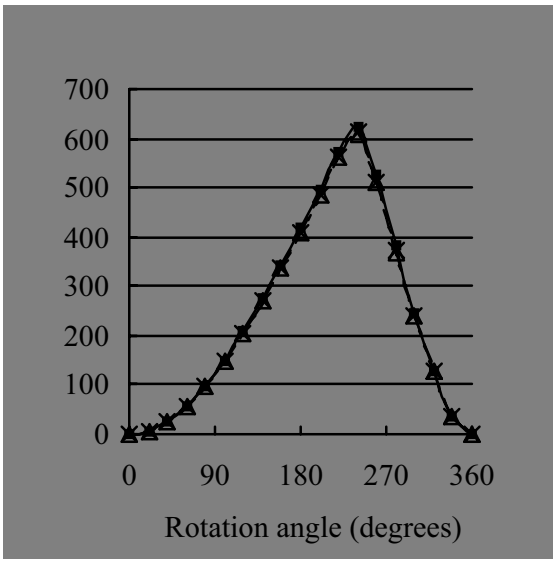

Figure 7 : Axial force of the middle element

7 Conclusion

The element coordinates were defined from the energy principle, and the end deformations in the coordinates became geometrically clear. Consequently, the end deformation can be exactly expressed by treating finite rotation with geometric strictness, and the geometric stiffness is derived from expansion of the end deformations by nodal displacement.

In a computational example, even if using the simple expression based on the beam-column theory and using small number of elements, the equilibrium solution has sufficient accuracy.

References

Bathe, K. J; Bolourch, S (1979): Large displacement analysis of three-dimensional beam structures. *Int. J. Numerical Method of Engg.*, Vol. 14, pp. 961-986.

Goto, H; Kuwataka, T.; Nishihara, T.; Iwakuma, T (2003): Finite displacement analysis using rotational degrees of freedom about three right-angled axes. *CMES: Computer Modeling in Engineering & Sciences*, Vol. 4, No. 2, pp. ?.

Goto, S (1983): A formulation of tangent geometric stiffness matrix for space structure. *Proc. of JSCE*, No. 335, pp. 1-12.

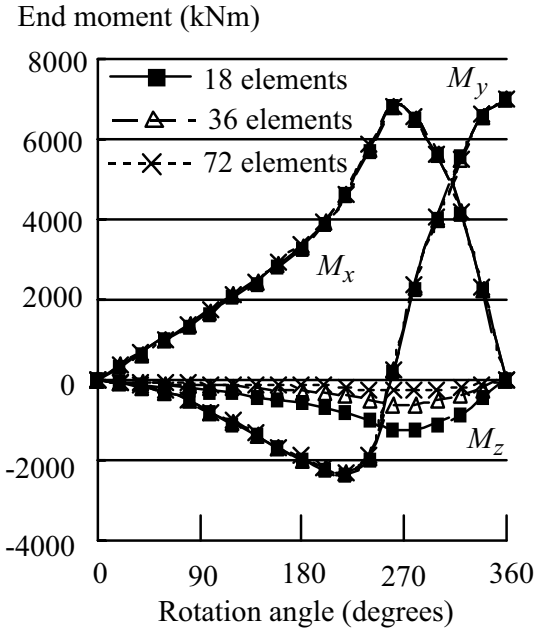

Figure 8 : End moment of the middle element

Goto, Y.; Hasegawa, A.; Nishino, F (1984): Accuracy and convergence of the separation of rigid body displacement for plane curved frames. *Proc. of JSCE*, No. 344, pp. 29-39.

Hsiao, K. M.; Lin, W. Y. (2003): A buckling and post-buckling analysis of rods under end torque and compressive load. *CMES: Computer Modeling in Engineering & Sciences*, Vol. 4, No. 2, pp–.

Iguchi, S; Goto, S; Ijima, K; Obiya, H (2001): Folding analysis of reversal arch by the tangent stiffness method. *Structural Engineering and Mechanics*. Vol. 11, No. 2, pp. 211-219.

Iguchi, S; Goto, S; Ijima, K; Obiya, H (1997): An analysis of spatial frame structures with finite rotation. *Proceedings of the Conference on Computational Engineering and Science*. Vol. 2, No. 2, pp. 451-454.

Iura, M.; Hirashima, M. (1985): Geometrically nonlinear theory of naturally curved and twisted rods with finite rotations. *Proc. of JSCE*, Vol. 2, No. 2, pp. 107-117.

Kassimali, A.; Abbasnia R. (1991): Large deformation analysis of elastic space frames. *Journal of Structural Engineering*, Vol. 117, No. 7, pp. 2069-2087.

Oran, C. (1973) Tangent stiffness in space frame. *ASCE*, Vol. 99, No. ST6, pp. 987-1001.

Zupan, D.; Saje, M. (2003): A new finite element formulation of three-dimensional beam theory based on interpolation of curvature. *CMES: Computer Modeling in Engineering & Sciences*, Vol. 4, No. 2, pp. ?.